

Type-I to Type-II Superlattice Transition in Strained Layers of $\text{In}_x\text{Ga}_{1-x}\text{As}$ Grown on InP

D. Gershoni, H. Temkin, J. M. Vandenberg, S. N. G. Chu, R. A. Hamm, and M. B. Panish

AT&T Bell Laboratories, Murray Hill, New Jersey 07974

(Received 14 July 1987)

Optical and electronic properties of $\text{In}_x\text{Ga}_{1-x}\text{As}$ strained-layer superlattices grown on InP have been investigated over the entire range of indium compositions, $0 < x < 1$. We demonstrate a type-I to type-II superlattice transition at $x \lesssim 0.20$. Below this critical concentration electrons become confined to the InP layer. Excellent agreement is obtained with a band-structure calculation based on empirical relative valence-band energies and deformation-potential theory. This agreement suggests that the effect of strain on these relative energies can be neglected.

PACS numbers: 73.20.Dx, 73.40.Kp

The energy-band lineups at semiconductor heterojunctions and the effects of strain on these lineups are of intense interest.¹⁻⁴ Strained-layer superlattices (SLS) are preferred for such studies since they offer high-quality interfaces at which the band gaps and strain can be varied over wide ranges. Particularly attractive is the normally lattice-matched $\text{In}_x\text{Ga}_{1-x}\text{As}$ -InP system in which the absolute magnitude, as well as the sign, of strain can be readily controlled as the layer composition is changed from $x=0$ (GaAs) to $x=1$ (InAs). Previous work on $\text{In}_x\text{Ga}_{1-x}\text{As}$ grown on GaAs does not permit the same degree of flexibility.⁵⁻⁷

The $\text{In}_x\text{Ga}_{1-x}\text{As}$ -InP SLS samples were grown by gas-source molecular-beam epitaxy^{8,9} on (100)-oriented InP substrates in a *p-i-n* configuration. The undoped superlattice was prepared on a 0.25- μm -thick *n*-InP buffer layer. It consisted of ten $\text{In}_x\text{Ga}_{1-x}\text{As}$ quantum wells with thicknesses ranging from 20 to 100 Å, in different samples, separated by ≈ 300 -400-Å-thick InP barriers. The indium concentration x was varied from $x=0$ (GaAs) to $x=1.0$ (InAs). The superlattice was overgrown with 0.3 μm of *n*-InP and 1 μm of *p*-InP, thus placing the *p-n* junction within the larger-band-gap InP. Nine samples were studied, one lattice matched with $x=0.53$, three with $x > 0.53$, i.e., compressed biaxially, and the remainder under tension ($x < 0.53$). The well thicknesses and strain were determined by our fitting the satellite pattern in the (400) x-ray diffraction scans with a kinematic step model simulation described previously.^{10,11} The structural information thus provided agrees very well with estimates based on the growth parameters as well as transmission electron microscopy (TEM). TEM cross sections of samples with ternary strained layers show defect-free superlattices with very sharp well-barrier interfaces. At $x=0$ (31-Å well widths) and $x=1$ (20-Å well widths) a periodic distribution of dislocation tangles ≈ 800 Å wide was observed. The regions between the dislocation tangles with an average distance of 800 Å ($x=0$) and 1400 Å ($x=1$), however, contain defect-free quantum wells with perfect interfaces. The mismatch strain at those regions is therefore unrelaxed.

The presence of dislocations in these two samples is not surprising since their layer thicknesses exceed the critical layer thickness¹² (16 Å for GaAs/InP, 20 Å for InAs/InP). Their density is sufficient to degrade the luminescence intensity and the satellite pattern in the x-ray diffraction, but not the photocurrent signal, which is less sensitive to crystal imperfections.

Figure 1 presents photocurrent response spectra for six samples with $0 < x < 0.64$. With use of the unbiased *p-i-n*'s in a waveguide geometry, the traces represent the TE (i.e., incident light polarized parallel to the SLS layers, solid line) and TM (dashed line) polarization. The

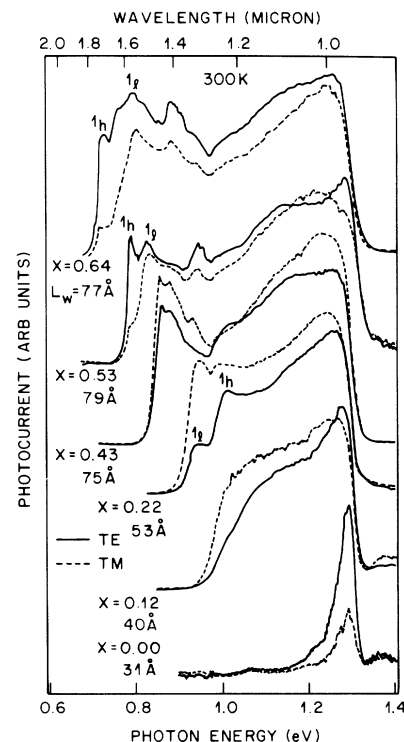


FIG. 1. Polarized photocurrent spectra of the waveguide structures.

two spectra allow us to distinguish between the light- and heavy-hole-electron transitions because of a dipole selection rule which prohibits the heavy-hole transition in the TM and favors it in the TE polarization.¹³ The waveguide efficiency decreases at higher energies and the photoresponse of all the samples is cut off above 1.32 eV, close to the InP band edge. Even at 300 K we observe the $n=1$ heavy and light excitons switching their relative positions for $x < 0.44$, so that the light hole becomes the lowest-energy state as discussed previously.⁹ Another striking phenomenon is the vanishing of the exciton structure for In concentration lower than $x \approx 0.20$ and a complete disappearance of the SLS response for the $x=0$ sample. Similarly, while very intense low-temperature exciton photoluminescence is observed in samples with $x > 0.2$, this signal disappears at lower In concentrations.⁹ These changes are not associated with the increased defect density. First, the absence of the photoluminescent response and a different photocurrent response are observed in the sample with $x=0.12$ which we consider, on the basis of x-ray diffraction and TEM, to be of very high quality. Second, a normal photocurrent response is observed in a sample with $x=1$, which exhibits a defect density similar to the $x=0$ sample. These effects are explained below by the transition from type-I (quantum well in both the valence and conduction bands) to type-II (quantum well in the valence band and a potential barrier in the conduction band) superlattice at In concentrations below $x \approx 0.2$.

Commensurate growth of strained $\text{In}_x\text{Ga}_{1-x}\text{As}$ on (100)-oriented InP results in in-plane biaxial strain. The strain epitaxial layers experience a tetragonal distortion, resulting in a very simple form of the strain tensor e_{ij} .^{13,14} The e_{zz} element of the strain tensor, where z is taken along the growth direction, can be obtained directly from the x-ray diffraction measurements. With use of Vegard's law, elastic theory, and the known binary stiffness coefficients,¹⁵ the composition can be then determined to better than 1%. The strain effect on the lowest conduction and the highest valence bands can be calculated with the phenomenological deformation-potential theory.¹⁴ We have used the conduction-band hydrostatic deformation potentials for InAs and GaAs as calculated by Camphausen, Nevill Connell, and Paul.¹⁶ While the GaAs value is in agreement, to within the experimental error, with the most recent measurements of Nolte, Walakiewicz, and Haller,¹⁷ the calculated energies are not very sensitive to this parameter. For the determination of the valence-band offset between the strained layer and InP, we use the relative valence-band energies obtained by Bauer and Margaritondo.³ The calculated band structure of the strained layers as a function of x is plotted in Fig. 2. The energy scale in this figure is referenced to the InP valence band and the arrows indicate excitonic transitions experimentally determined from the data of Fig. 1, except for the two points with the lowest x

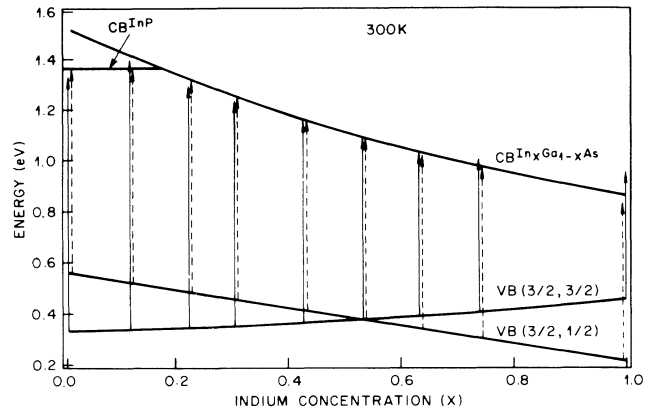


FIG. 2. Calculated band structure of the strained layers. Energy is referenced to the InP valence band. Arrows indicate transitions corrected for the quantum size effect. Data for two samples with the lowest x were obtained under applied electric field.

values which have been obtained under bias, as discussed below. The transition energies are also referenced to the valence band calculated for a given In concentration and corrected for the appropriate quantum size effect with the parameters of Ref. 15.¹⁰ The conduction band of InP is indicated by a straight horizontal line. Remarkably good agreement is obtained between the calculated energy bands and the experimental data points for the entire range of $0.2 < x < 0.74$. In the $x=1.0$ sample, we observe misfit dislocations indicating some strain relaxation resulting in reduced $\text{VB}(\frac{3}{2}, \frac{3}{2})-\text{VB}(\frac{3}{2}, \frac{1}{2})$ splitting. However, the data points at the low extreme of In concentration, $x < 0.2$, clearly cannot be interpreted as transitions between the conduction-band electrons and valence-band light and heavy holes of the strained-layer quantum well. These data points fit only transitions between the unstrained conduction band of the InP barrier and the strained-layer valence bands. Further evidence for this interpretation is obtained from the bias dependence of the photocurrent spectrum. The response spectra of the three samples with the low In concentration for different values of applied voltage are plotted in Fig. 3. For the sample with $x=0.30$, there is almost no change in the shape of the photocurrent spectrum as the bias is increased from 0 to 6 V, corresponding to a field of 10^5 V/cm, applied across the superlattice. This behavior is typical of all the samples with $x > 0.20$ where the only noticeable spectral change with bias was a slight down shift in the energy of the $1s$ exciton due to the quantum confined Stark effect.¹⁸ In contrast, while in samples with $x < 0.20$, no excitons could be seen without external bias, even low applied field causes dramatic changes. The SLS response becomes visible at bias levels as low as 0.2 V. At higher bias levels the photocurrent response begins to resemble that of the samples with much higher

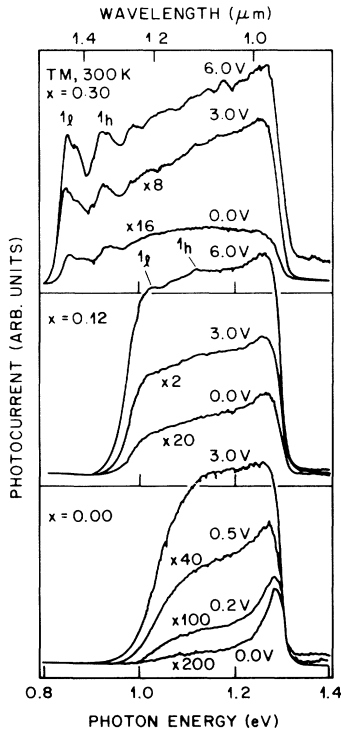


FIG. 3. Reverse-bias dependence of the photocurrent response spectra for three samples with low In concentrations.

x . The excitonlike structure could be seen in the $x=0.12$ sample under a bias of 6 V.

The spectral changes illustrated in Fig. 3 can be explained semiquantitatively in terms of changing overlap between the hole and electron wave functions for $n=1$ states of a type-II superlattice. The wave functions were calculated with the resonant tunneling method¹⁸ and we assume that the strength of the excitonic transition is proportional to the square of their overlap integral.¹⁹ For $x > 0.2$, both electrons and holes are confined in the strained layers of $\text{In}_x\text{Ga}_{1-x}\text{As}$, forming a structure known as a type-I superlattice. The effect of the external electric field on the probability distribution of these particle states is the decreased overlap as the electron and hole distributions are pulled apart and a slight energy shift due to the quantum confined Stark effect. This last effect is very small, less than 10 meV.²⁰ The photocurrent spectrum obtained under a bias of 3 V does not show significant changes as the square of the overlap integral (calculated for the $x=0.30$ sample) decreases from 0.94 to 0.80. This minor change is not detectable and the measured photocurrent actually increases as a result of a larger depletion width. The electric-field effect is dramatically different in a type-II superlattice, as shown in Fig. 4. The normalized $n=1$ sublevel probability distributions for electrons and light holes are shown to scale together with the quantum-well energy

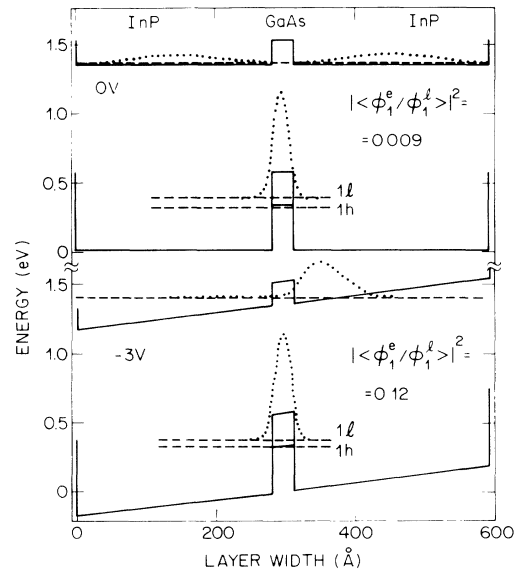


FIG. 4. Calculated quantum-well energy structure and wave functions of the electrons and light holes in type-II superlattice $x=0.0$ sample with and without applied electric field.

structure. In the absence of applied field the probability distributions of electron and holes are spatially separated with the resulting overlap of less than 0.009. The electrons are confined to the 280-Å-wide InP wells with the calculated depth of 172 meV below the strained GaAs barriers. The light holes are still confined in the strained layer. As discussed above, the transitions between these states are not observed in either the photocurrent or luminescence spectra. The application of the electric field to this type of superlattice results in a dramatic increase of the calculated overlap, to 0.12, which manifests itself in a large increase of the photocurrent response. However, in order to account quantitatively for the observed spectral change, higher-order exciton states, as well as continuum states, should be included in the calculations.¹⁹ With increased bias, the wave function of an electron quasiconfined to InP penetrates further into the strained-layer barrier which gives rise to discernible exciton resonances. This effect is more pronounced for the sample with $x=0.12$, in which the InGaAs potential barrier is lower.

In the absence of direct experimental data, the electronic bands of the strained InGaAs, plotted in Fig. 2, were obtained by the linear interpolation of the relative valence-band energies of the unstrained binary compounds compiled in Ref. 3 ($\Delta E_V^{\text{InAs/InP}}=0.41$ eV, $\Delta E_V^{\text{GaAs/InP}}=0.34$ eV). This procedure therefore ignores the effect of strain on the relative valence-band energies which, according to midgap theories,^{1,2} should arise from the strain-induced shift of the midgap point. The In concentration at which the superlattice switches from type I to type II is a sensitive function of the relative (un-

strained) GaAs/InP valence-band energy. For instance, a 100-meV change in the value of this parameter, from 0.34 to 0.24 eV, results in the critical In concentration shifting from $x_c = 0.195$ to $x_c = 0.088$. A change of 170 meV, in the same direction, would eliminate the transition. Experimentally, the transition point can be determined to lie in the range of $0.15 < x < 0.22$, corresponding to ± 60 -meV error in the relative valence-band energy. The agreement suggests that the effect of strain on $\Delta E_V^{\text{GaAs/InP}}$ is vanishingly small.

In summary we have studied the $\text{In}_x\text{Ga}_{1-x}\text{As-InP}$ SLS for the entire range of In concentration $0 < x < 1$. The trend of optical measurements shows a transition at $x \approx 0.2$, which we attribute to the change from a type-I to type-II superlattice. This is supported by the bias dependence of the spectral response and is in agreement with calculations based on elastic and phenomenological deformation-potential theories. We find no evidence for a strain dependence of the relative valence-band energies.

¹J. Tersoff, Phys. Rev. Lett. **12**, 2755 (1986).

²M. Cardona and N. E. Christensen, Phys. Rev. B **35**, 6182 (1987).

³R. S. Bauer and G. Margaritondo, Phys. Today **40**, No. 1, 27 (1987).

⁴Proceedings of the Thirteenth Annual Conference on the Physics and Chemistry of Semiconductor Interfaces, Pasadena,

California, 1986, edited by R. S. Bauer, J. Vac. Sci. Technol. B **4**, No. 4 (1986).

⁵J. Y. Marin, M. N. Charasse, and B. Sermage, Phys. Rev. B **31**, 8298 (1985).

⁶I. J. Fritz, J. J. Drummond, G. C. Osburn, J. E. Schirber, and E. D. Jones, Appl. Phys. Lett. **48**, 1678 (1986).

⁷J. Menendez, A. Pinczuk, D. J. Werder, S. K. Sputz, R. C. Miller, D. L. Sivco, and A. Y. Cho, unpublished.

⁸M. B. Panish, Prog. Cryst. Growth Charact. **12**, 1-28 (1986).

⁹D. Gershoni, J. M. Vandenberg, R. A. Hamm, H. Temkin, and M. B. Panish, Phys. Rev. B **36**, 1320 (1987).

¹⁰J. M. Vandenberg, R. A. Hamm, M. B. Panish, and H. Temkin, J. Appl. Phys. **62**, 1278 (1987).

¹¹J. M. Vandenberg, S. N. G. Chu, R. A. Hamm, M. B. Panish, and H. Temkin, Appl. Phys. Lett. **49**, 1302 (1986).

¹²J. W. Matthews and A. E. Blakeslee, J. Cryst. Growth **27**, 118 (1974).

¹³J. C. Hensel and G. Feher, Phys. Rev. **129**, 1401 (1963).

¹⁴G. L. Bir and G. E. Pikus, *Symmetry and Strain Induced Effects in Semiconductors* (Halsted, United Kingdom, 1974).

¹⁵S. Adachi, J. Appl. Phys. **53**, 8775 (1982).

¹⁶D. L. Camphausen, G. A. Nevill Connell, and W. Paul, Phys. Rev. Lett. **26**, 184 (1971).

¹⁷D. D. Nolte, W. Walakiewicz, and E. E. Haller, Phys. Rev. Lett. **59**, 501 (1987).

¹⁸D. A. B. Miller, D. S. Chemla, J. C. Damen, A. C. Gossard, W. Wiegman, T. H. Wood, and C. A. Burrus, Phys. Rev. B **32**, 1043 (1985).

¹⁹D. A. B. Miller, J. S. Weiner, and D. S. Chemla, IEEE J. Quantum Electron. **22**, 1816 (1986).

²⁰H. Temkin, D. Gershoni, and M. B. Panish, Appl. Phys. Lett. **50**, 1776 (1987).